Biosensors and Bioelectronics 122 (2018) 121–126

Contents lists available at ScienceDirect

Biosensors and Bioelectronics

journal homepage: www.elsevier.com/locate/bios

Aptamer functionalized MoS_2-rGO nanocomposite based biosensor for the detection of Vi antigen

Preeti Kumari Pathania[a,b], Jai Kumar Saini[a,b], Shania Vij[b], Rupinder Tewari[b], Priyanka Sabherwal[c,*], Praveen Rishi[b,*], C. Raman Suri[a,*]

[a] CSIR-Institute of Microbial Technology, Sector 39A, Chandigarh 160036, India
[b] Department of Microbiology, Panjab University, Chandigarh 160014, India
[c] Institute of Nanoscience and Technology, Habitat Center, Phase 10, Mohali 160062, India

ARTICLE INFO

Keywords:
Aptamers
MoS_2-rGO nanocomposite
Square wave voltammetry (SWV)
Ferrocene-boronic acid
Vi capsular polysaccharide

ABSTRACT

We report a novel aptamer functionalized MoS_2-rGO based electrochemical method for Vi polysaccharide antigen mediated detection of enteric fever. Herein, highly selective anti-Vi aptamers were screened from a pool of oligonucleotides using a microtitre based SELEX approach and characterized for its specificity and stability. The MoS_2-rGO nanocomposite was synthesized using a liquid assisted exfoliation by taking optimum ratio of MoS_2 and rGO. The nanocomposite presented synergistic effect owing to easy biomolecular functionalization and enhanced conductivity. The screened anti-Vi aptamers were embedded on the MoS_2-rGO nanocomposite via thiol linkage to give a stable biointerface. The developed aptasensor was characterized and further evaluated for its performance with different concentrations of Vi antigen using ferrocene labeled boronic acid as an electroactive probe. The aptasensor responded linearly in the range between 0.1 ng mL^{-1} to 1000 ng $mL^{-1}$with a detection limit of 100 pg mL^{-1}, and did not show any cross-reactivity with other bacterial polysaccharides indicating high specificity. The applicability of the developed aptasensor was further validated in urine and sera specimens spiked with Vi antigen.

1. Introduction

Enteric fever caused by *Salmonella enterica* serovar Typhi or serovars Paratyphi A, B and C remains a life threatening systemic infection. It is a major health problem in developing countries. It represents approximately 17–22 million cases leading to 0.2–0.6 million deaths every year as per WHO records (WHO, 2017). Detection of *Salmonella* is challenging as the infection can result into diverse clinical manifestations that overlap with wide spectrum of other diseases (Mutreja et al., 2016). Detection strategies based on blood culture is not only time consuming but the results are also compromised if the antimicrobial agents are consumed by the patient prior to sampling (Kishore et al., 2014). On the other hand, routinely employed Widal test performs well but is again time consuming. Moreover, Widal test as well as other tests recently made available commercially such as Tubex and Typhidot carry many shortcomings, as the sensitivity, specificity and prediction values differ in different geographical areas. Therefore, these tests are difficult to interpret in areas where typhoid fever is endemic (Pandey et al., 2012, 2014). As no non-cultural test for typhoid fever has been consistently found to be sufficiently sensitive and specific, most of the laboratories still rely upon Widal test (Pandey et al., 2012). Therefore, there is a need to develop a fast, reliable, and easy to perform diagnostic test for *S.* Typhi which is highly selective and sensitive.

Out of the commonly occurring infections caused by *Salmonella* species, *S.* Typhi carries a Vi capsular polysaccharide (Vi antigen) which has been reported to increase the infectivity (Robbins and Robbins, 1984) and severity of the disease due to its anti-phagocytic activity and to endow the organism to have resistance towards oxidative stress (Hornick et al., 1970; Looney and Steigbigel, 1986; Sharma and Qadri, 2004). It is reported to be expressed at low and medium osmolarity in the hosts and serves to protect bacterial cells from complement mediated actions of O antigen specific antibody (Wilson et al., 2011; Robbins and Robbins, 1984). These characteristics of Vi antigen make it an appropriate target for the detection of typhoidal Salmonellosis. Though Vi antigen is present in *Salmonella* Paratyphi C, but its incidence is very low as compared to that of serovar Typhi (John et al., 2016). Vi antigen is also present in *Salmonella* Dublin and *Citrobacter freundii,* but the clinical manifestations caused by these organisms do not overlap with the enteric fever (Nayar et al., 2014; Mohammed et al., 2017). Thus, presence of Vi is primarily limited to *S.* Typhi and helps in

* Corresponding authors.
E-mail addresses: psnanobiotech@gmail.com (P. Sabherwal), rishiparveen@pu.ac.in (P. Rishi), crsuri58@gmail.com (C.R. Suri).

https://doi.org/10.1016/j.bios.2018.09.015
Received 21 May 2018; Received in revised form 25 August 2018; Accepted 3 September 2018
Available online 05 September 2018
0956-5663/

differentiating it from other commonly occurring enteric pathogens (Pandey et al., 2012) such as *S.* Typhimurium and *E. coli*.

Earlier we have reported detection of Vi antigen using anti Vi antibody functionalised gold nanoparticles or CdTe quantum dots bioprobes with the detection limit of 5 ng and 1 ng of Vi antigen respectively (Pandey et al., 2012; Pandey et al., 2015). Due to the advent of newer technologies, efforts are continuously being made to increase the sensitivity and specificity. In the present study, we have focussed on anti-Vi aptamers rather than anti-Vi antibodies because aptamers are known to be more stable and their production is time and cost effective (Jayasena, 1999; Houwena and Kageb, 2012). Moreover, aptamers are best suited when an antigen is not strongly immunogenic such as Vi antigen. Therefore, use of aptamer in electrochemical techniques including cyclic voltammetry (CV), square wave voltammetry (SWV) and differential pulse voltammetry (DPV) has been widely accepted given their simplicity, sensitivity and specificity for the detection of low levels of disease biomarkers (Meirinho et al., 2016).

Recent developments in electrochemical biosensors are focussed on the transition metal dichalcogenides (TMDs) mainly Molybdenum disulfide (MoS_2) due to their tunable band gap, enhanced electrical, optical and thermal properties (Gao et al., 2017). However, they represent problems of restacking due to their minimised surface energies and also have low intrinsic conductivity. These shortcomings can be overcome by using rGO or graphene based nanomaterials which improve the electronic conductivity as well as prevent restacking of these TMDs (Rao et al., 2009; Wang et al., 2014). The current work thus envisaged the advantages of high selectivity of anti-Vi aptamers functionalized 2D MoS_2-rGO nanocomposite using ferrocene boronic acid as an electroactive probe for voltammetric detection of Vi antigen (Fig. 1)

2. Experimental section

2.1. Materials

The HPLC purified DNA library 5′-ATCCAGAGTGACGCAGCA-(N45)-TGGACACGGTGGCTTAGT-3′ was synthesized from Sigma, India as also described in previous studies (Pathania et al., 2017; Sefah et al., 2010). The primers were labeled at the 5′ end with FITC/Thiol for monitoring the progression of selection rounds and antisense strand was labeled at the 5′ end with biotin. The sequences of the designed primers were: 5′-FITC/Thiol-ATCCAGAGTGACGCAGCA-3′ and 5′-biotin-ACTAAGCCACCGTGTCCA-3′. PCR Master mix and PCR tubes were purchased from Thermo Scientific (India). Bovine serum albumin, streptavidin, glycine, hydrazine hydrate, graphene, potassium ferricyanide and potassium ferrocyanide, ferrocene-boronic acid (FBA) and N-methyl pyrollidine (NMP) were purchased from Sigma-Aldrich (India). MoS_2 bulk was purchased from Alfa-aesar. All other chemicals used in the study were of analytical grades obtained from Merck India.

2.2. Generation and characterization of anti-Vi aptamers using plate based SELEX

The ssDNA aptamers were screened from a library of oligonucleotides with a random region of 45 nucleotides flanked by constant

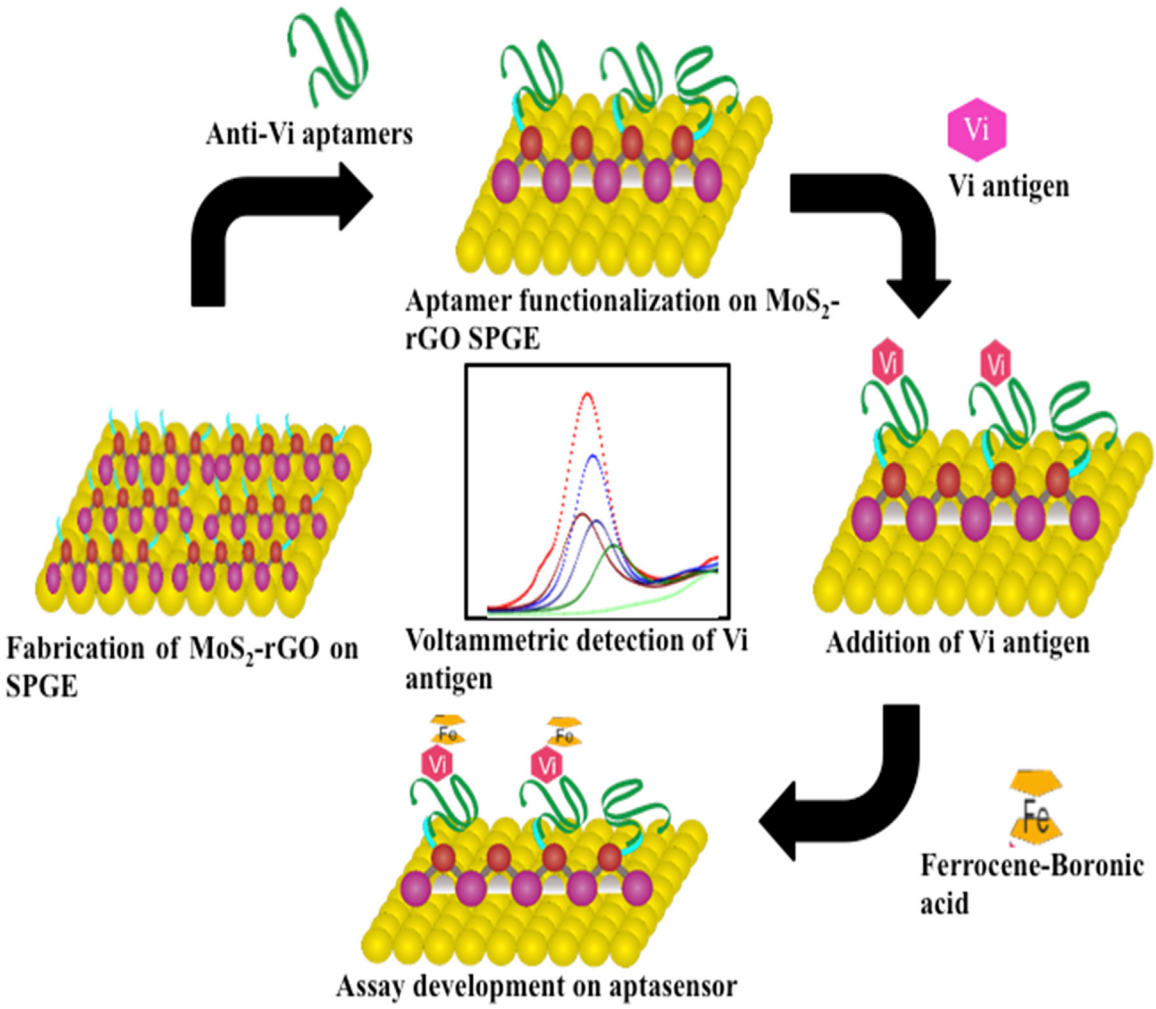

Fig. 1. Schematic illustration of aptamer functionalized 2D MoS_2-rGO nanocomposite based biosensor for the detection of Vi antigen.

primer-binding region of 18 nucleotides via microtitre based SELEX approach. Briefly, 10 μg mL^{-1} of BSA-Vi conjugate prepared as per our previous protocol (Pandey et al., 2014) was dissolved in 50 mM carbonate buffer pH 9.6 and coated on a micro titer plate overnight at 4 °C followed by exposure with preheated ssDNA library (10^{14} molecules) for 2 h at 37 °C. The target bound ssDNA population was then eluted via glycine-HCl followed by PCR amplification and nanobioprobe mediated ssDNA generation. These selected ssDNA was used for next SELEX round. A total of 6 positive rounds of SELEX with BSA-Vi and a negative round with BSA was performed. The quality and quantity of screened aptamers was monitored by agarose gel electrophoresis and Nanodrop (Thermo Scientific ND1000). All the steps followed for elution, PCR amplification, ssDNA generation and electrophoresis studies have been detailed in supplementary information S1A. Binding studies of the screened aptamers with target molecule was determined using FITC labeled Vi aptamer based direct fluorescence method on a microtitre plate using graph prism pad software (version 7.0) via a linear fit model. Selectivity of the aptamer was also supported via confocal studies done with Vi expressing *S*. Typhi cells along with other enteric pathogens expressing different polysaccharides as detailed in supplementary information S1B.

2.3. Synthesis and characterization of 2D MoS_2-rGO nanocomposite

A top down approach based on liquid mediated exfoliation was performed for the synthesis of 2D MoS_2-rGO nanocomposite. In brief, MoS_2 and rGO structures were synthesized by the method reported earlier (Coleman et al., 2011; Kumar et al., 2015) as detailed in supplementary information S2. Thereafter, 10 mg of as prepared MoS_2 dots were added to 2.5 mg of rGO dropwise under continuous stirring in 10 mL NMP(4:1 ratio) and the mixture was ultra-sonicated for 1 h at room temperature (RT) using a probe sonicator (35% amplitude, 15 s ON, 15 s OFF 750 W). The resulting dispersion was centrifuged at 12,000 rpm and washed thoroughly with ethanol and distilled water. The morphological analysis of prepared MoS_2 and MoS_2-rGO nanocomposite was carried out by Transmission electron microscopy (TEM) (using Model JEM-2100 Tem 200 kV). Microstructural analysis was investigated via different vibrational modes of carbon-carbon and metal-sulphur bonds using Raman Spectrophotometer 785-HP-NIR laser (1.5 eV). The spectra of first order Raman scattering for rGO, MoS_2 and 2D MoS_2-rGO nanocomposite were also observed.

2.4. MoS_2-rGO nanocomposite based aptasensor development

Screen printed gold electrodes (SPGE) (Drop sense DS 220AT) were used for electrochemical studies and for aptasensor development. Electrochemical studies were carried out (using EC workstation CHI660D) by drop casting optimized concentration (conc.) 12.5 μg of the prepared MoS_2-rGO nanocomposite as mentioned above) on the working area of gold electrodes and dried for 2 h at 40 °C. The MoS_2-rGO nanocomposite coated electrodes were then assessed for their electrochemical performance using cyclic voltammetry (CV), Electrochemical impedance spectroscopy (EIS) and SWV techniques as detailed in supplementary information S3. The well-characterized MoS_2-rGO fabricated electrodes were used for biointerface development. Briefly, 10 μg of specific anti-Vi aptamers was dropcasted on the working area of as prepared electrodes and kept for 1 h incubation at 37 °C. Assessment of biointerface development, stability and robustness of prepared electrodes were studied using electrochemical measurements including cyclic voltammetry (CV) and square wave voltammetry (SWV) on an electrochemical workstation (CH Instruments 660D, TX, USA) using a redox couple (5 mM $[Fe(CN)_6]^{3-/4-}$) solution prepared in 10 mM PBS (pH 7.4) at RT. All the electrochemical studies were repeated thrice with 5 different electrodes.

2.5. Vi antigen detection and selectivity of aptasensor

SWV technique was employed with the developed aptasensor for the detection of Vi antigen. For bioassay development, varying amount of Vi antigen (0.1 ng mL^{-1} to 1000 ng mL^{-1}) was incubated on developed aptasensors for 30 min each followed by washing and incubation with 5 mM solution of FBA for the estimation of Vi antigen. Boronic acid is also termed as boron-lectins due to their lectin like properties of multivalent saccharide binding via interacting with cis 1,2 diols and cis 1,3 diols to form a five or six membered cyclic esters that enhances both the specificity as well as selectivity, making boronic acid saccharide sensing possible at nM to mM range (Wu et al., 2013). The generated ferrocene current was measured using SWV and the Ferrocene oxidation current was plotted versus Vi conc. in linear fit method to calculate the regression coefficient and limit of detection (LOD). The selectivity of the aptasensor was also investigated with different polysaccharides of bacterial origin using LPS from *E. coli, S.* Typhimurium, *S.* Typhosa and hexuronic acid (Building block of capsular antigen of *E. coli*). All the experiments were performed thrice (n = 3) with five different screen-printed electrodes.

2.6. Applicability of the aptasensor in biological specimens

The performance and applicability of the aptasensor was demonstrated using sera and urine specimen. Samples were collected from healthy individuals (who have not suffered from any infection caused by organisms expressing Vi antigen) and processed as detailed in supplementary information S4. These specimen were spiked with different conc. of Vi antigen (100 ng mL^{-1}, 10 ng mL^{-1} and 1 ng mL^{-1}) separately, and were added onto the aptamer functionalized electrodes for assay development by recording the SWV scans to check the interference due to other non-specific components of specimen. The recovery studies for Vi antigen spiked in serum and urine were performed by standard recovery protocol as mentioned below:

$$\text{Percentage recovery} = \frac{\text{Conc. of Vi in spiked sample}}{\text{Conc. of Vi spiked diluent(PBS)}} *100.$$

3. Results and discussion

3.1. Generation and characterization of anti-Vi aptamer via modified SELEX

Aptamers are good alternatives of antibodies due to their ease of selection, stability, specificity, lesser batch-to-batch variation, and their higher affinity as compared to antibodies (Sharma et al., 2013). The quality and quantity of the screened aptamers after each iterative round as per the OD measured at 260 nm, 260/280 and 260/230 ratio (Table S1 Supplementary information) represent high purity of the screened binders and also depicts an increase in the amount of DNA progressively with each successive round which becomes constant after 6^{th} round of SELEX (Fig. 2A) indicating thereby enrichment of Vi binding aptamer population. As shown in Fig. S1 A, 2.5% agarose gel electrophoresis of ssDNA aptamer showing a single band slightly above the corresponding 50 bp standard ladder also confirms the purity. The binding affinity constant K_d of screened anti-Vi aptamers population was evaluated using Scatchard plot (saturation binding assay) by incubating the increasing amount of FITC labeled Vi aptamer (0.1–10,000 nM) on the microtitre plate as detailed in S1B and the calculated affinity constant K_d was found to be 638.6 nM, using a non-linear fit model. Binding studies and specificity of screened aptamers also supported the selectivity and binding of Vi antigen expressing *S*. Typhi cells but not with the polysaccharides of other closely related pathogens via confocal microscopy as demonstrated in Fig. S1B.

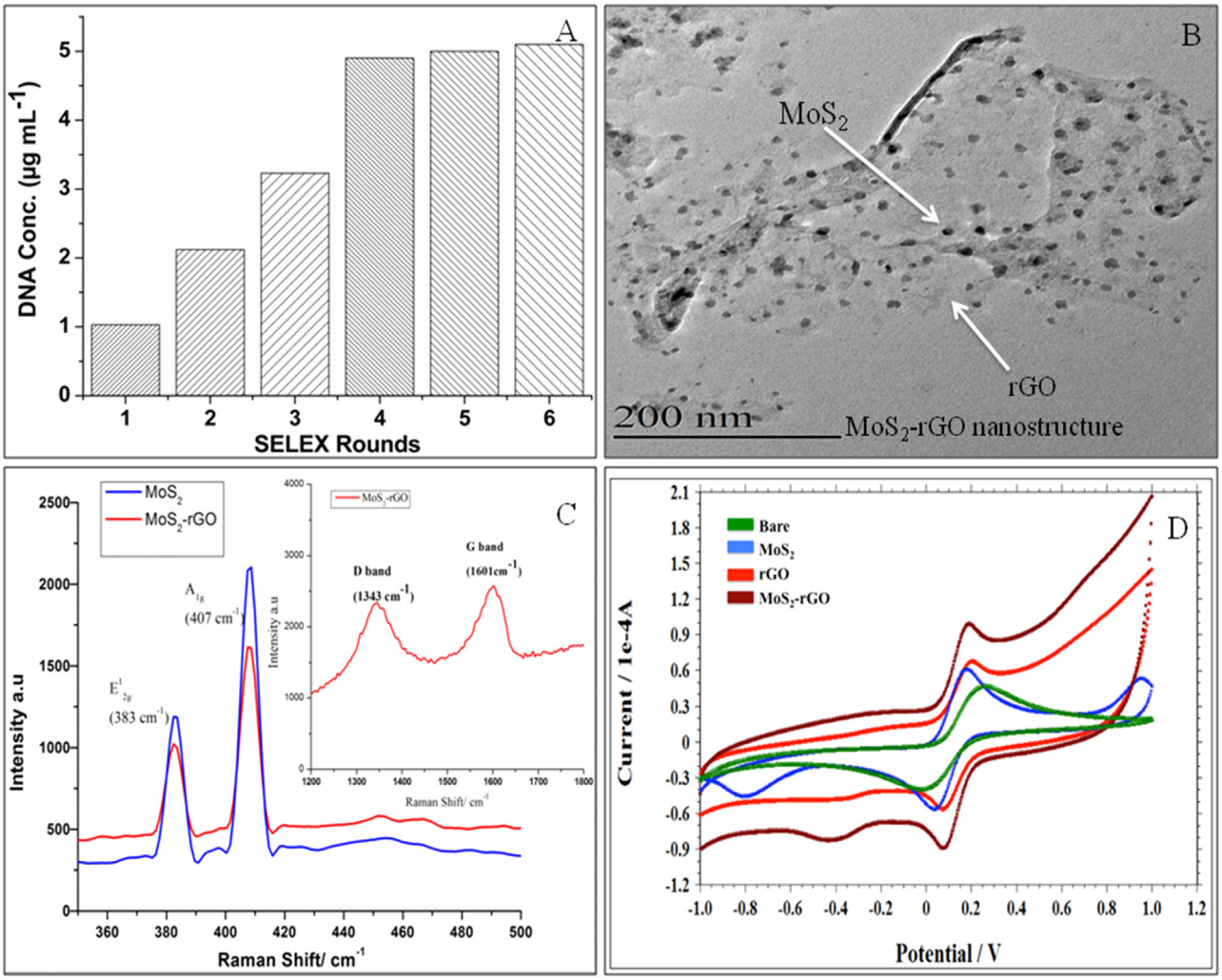

Fig. 2. (A) Spectroscopic characterization of different SELEX rounds (B) TEM image of the MoS_2-rGO nanocomposite (C) Raman spectra of the 2D MoS_2-rGO nanocomposite conjugate (D) CV scan of bare, rGO, MoS_2 and MoS_2-rGO modified electrodes.

3.2. MoS_2-rGO nanocomposite synthesis and characterization

Hybridizing MoS_2 and rGO via liquid phase exfoliation method offers high prospects to explore the properties of both the nanomaterials collectively owing to better properties like enhanced conductivity and ease of bio-molecular functionalization (Sahu and Mitra, 2015; Loan et al., 2014). In the current study, UV–VIS absorption spectra of exfoliated MoS_2 has been shown in Fig. S2A, depicting two characteristic excitonic absorption bands at 623 and 674 nm which is in agreement with the earlier report (Coleman et al., 2011). Structural and morphological characterization of MoS_2 and rGO has been detailed in Fig. S2 B-D. Individually, these nanostructures represent the problem of agglomeration in order to minimize their high surface energies (Rao et al., 2009; Wang et al., 2014). Therefore, hybridizing these materials with rGO or graphene based materials is good way to overcome the problem of restacking and increase method as described in our previous protocol (Sharma et al., 2013). The TEM analysis of synthesized MoS_2-rGO dispersion revealed rGO sheets decorated with MoS_2 nanocomposites (Fig. 2B) that may be due to vander wall stacking among them. This interaction could be helpful to avoid restacking of MoS_2 by lowering the surface energies and may thus exhibits collective properties of both the nanomaterials. The structural aspects of the MoS_2-rGO nanocomposite was studied using RAMAN scans (Fig. 2C) which showed characteristic MoS_2 peaks at 321 and 407 that corresponds to E^1_{2g} linked opposite vibration due to two S atoms with respect to Mo atom and A_{1g} peak originated from out plane vibrations of S atoms while two additional peaks were observed in the hybridized nanomaterials which corresponds to the D and (1343 cm^{-1}) and G (1601 cm^{-1}) bands because of the defects in sp^2 hybridized carbon of rGO due to in-plane and out-plane vibrations. Also, the different positions of rGO-MoS_2 depict a shift in higher wave number as compared to MoS_2.The electrochemical performance of the resulting MoS_2-rGO dispersion was assessed using CV and EIS studies, which revealed that the synthesized nanocomposite exhibits collective properties of both nanocomposite attributed to the properties like enhanced conductivity, increased surface area after fabrication of 2D MoS_2-rGO as compared to MoS_2, rGO and bare as shown in Fig. 2D which depicts maximum signal obtained after MoS_2-rGO functionalization. The stability of the as fabricated electrodes were checked by performing CV scan from 10 mV s^{-1} to 100 mV s^{-1} which shows that the process is under diffusion control as the current increases linearly on increasing the scan rate (Srivastava et al., 2011) as shown in S3B.

3.3. Aptamer functionlized MoS_2-rGO SPGE for electrochemical detection of Vi antigen

Aptamer based voltammetric electrochemical techniques such as CV, DPV and SWV have been employed as they confer advantages like low related noise, providing reliable and reproducible response for the quantification of a target molecule, endowing higher sensitivity and

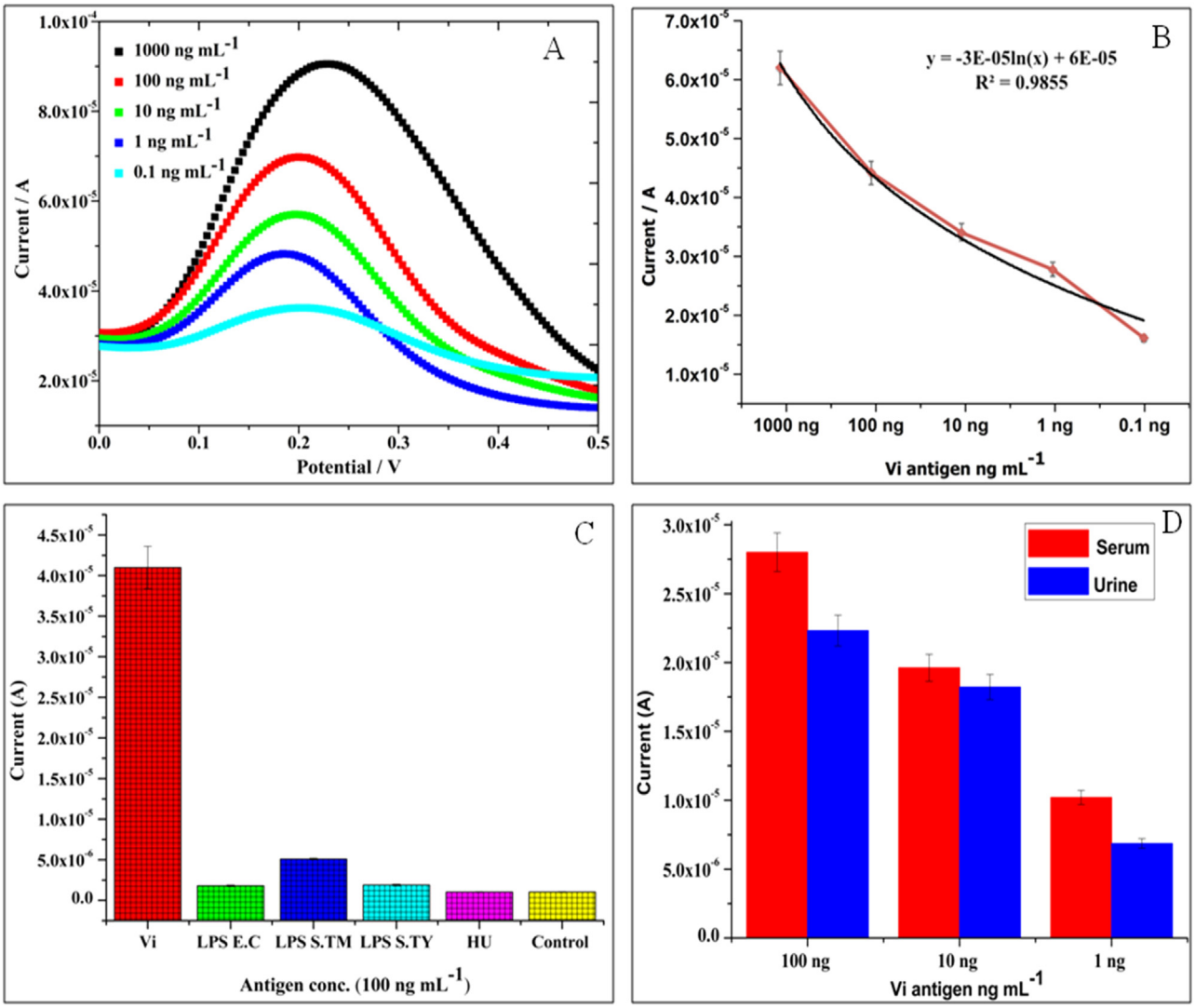

Fig. 3. (A) SWV spectra showing a linear response of the aptasensor with increasing the conc. of Vi antigen in PBS. (B) Linear plot for the standard Vi conc. (0.1–1000 ng mL^{-1}). (C) Specificity of the developed aptasensor with 100 ng mL^{-1} of different polysaccharides including Vi (Vi antigen from *S.* Typhi), LPS EC (*E. coli*), LPS S.TM (*S.* Typhimurium), LPS S.TY (*S.* Typhosa), HU (Hexuronic acid). (D) SWV scans of three different conc. (100, 10 and 1 ng mL^{-1}) of Vi antigen spiked urine and serum samples respectively.

specificity to the assay (Meirinho et al., 2016). These techniques further allow the detection of multiple compounds, which have different peak potentials thus offering the possibility of simultaneously detecting multiple analytes (Marks and Abdulhalim, 2015). In the present study, MoS_2-rGO fabricated platform was used for biomolecular functionalization of anti-Vi aptamers by drop-casting 10 µg of anti-Vi aptamer which depicted a decrease in current as shown in Fig. S 3A because of slight insulating behavior of anti-Vi aptamer clearly shown by increase in resistance after aptamer functionalization. The developed aptasensor also conferred high robustness that can be depicted from Fig. S3C which showed linear performance of aptasensor with increasing frequency (15–75 Hz) of SWV. For the development of an electrochemical assay, anti-Vi aptamer functionalized biointerface developed on the gold electrodes were incubated with different Vi antigen concentrations (0.1 ng mL^{-1} to 1000 ng mL^{-1}) in PBS for 30 min followed by incubation of FBA (5 mM) for 15 min. The current was recorded using Square Ware Voltammetry which showed that aptasensor responded linearly in a range of 1000 ng to 0.1 ng mL^{-1} showing high sensitivity with detection limit ~100 pg mL^{-1} (Fig. 3 A) which is higher than other existing method as mentioned in S5 (Table S2) Supplementary information, while the calculated R^2 value was 0.985 as shown in S4B. Control experiments were also done to ensure no peak current or any interference due to PBS as shown in Fig S4 C.

3.4. Selectivity and applicability of developed aptasensor

Gram-negative bacteria are known to express different polysaccharides on their surface with intra and interspecies variations. For example, LPS is present in all the Gram negative bacteria whereas K antigen (capsular polysaccharide) is yet another antigen expressed by *E. coli.* Therefore, assessment of cross-reactivity of developed sensing platform was performed with 100 ng mL^{-1} conc. of Vi antigen and LPS of *S.* Typhimurium, *E. coli* and *S.* Typhosa as well as with hexuronic acid. The recorded spectra in Fig. 3C represents negligible change in standard ferrocene oxidation peak current as compared to the same conc. of Vi antigen, suggesting very high selectivity of the developed platform. The applicability of proposed aptasensor was also validated using blood and urine specimens spiked with Vi antigen at three different concentrations (100, 10 and 1 ng mL^{-1}) as shown in Fig. 3D. The response was found to be linear with all the three concentrations, while the unspiked samples of urine and blood did not show any reactivity suggesting no interference due to other components present in the

samples (Fig S4C). However, the recovery rate in the Vi spiked serum and urine samples was lower (65.11% and 51.86% respectively) as compared to the standard sample (spiked in PBS). The low recovery might be attributed to the other charged moieties in the biological samples which tend to aggregate polysaccharides resulting in low availability of Vi for aptamer binding in bioassay. It has also been reported (Chaicumpa et al., 1992; Fadeel et al., 2004) that an uneven distribution and denaturation of the antigen in frozen and thawn urine specimens along with the intermittent release of antigen in urine of patients affect the sensitivity of the test. Due to the similarity in the Vi antigen of *S*. Paratyphi C, *S.* Dublin and *Citrobacter freundii* with *S*. Typhi Vi antigen, the developed platform may be employed to detect the infections caused by these organisms, if at all.

4. Conclusion

The present work demonstrates a novel electrochemical platform for Vi antigen based detection of enteric fever using a MoS_2-rGO nanocomposite and anti-Vi aptamer to increase the sensitivity and selectivity of the platform respectively. The developed aptasensor performed well in a range of 1000–0.1 ng mL^{-1} with the detection limit of 100 pg mL^{-1} in PBS, sera and urine sample with high selectivity towards Vi antigen. Additionally, this detection system might not only be helpful from epidemiological point of view for tracking the carriers harboring the organism carrying the antigen but also be used for the evaluation of prognosis of the disease after chemotherapeutic care of the patients. Though the validation of the device was done using spiked samples, its application needs to be evaluated in future using the real time clinical specimens.

Acknowledgements

The authors acknowledge Council for Scientific and Industrial Research (CSIR), India for providing Senior Research Fellowship (81253/2K15/1) to PKP. The authors also acknowledge Ms. Anjali (CSIR-IMTECH) for providing help in executing confocal experiments.

Appendix A. Supporting information

Supplementary data associated with this article can be found in the online version at doi:10.1016/j.bios.2018.09.015.

References

Chaicumpa, W., Ruangkunaporn, Y., Burr, D., Chongsa-Nguan, M., Echeverria, P., 1992. J. Clin. Microbiol. 30, 2513–2515.
Coleman, J.N., Lotya, M.,O., Neill, A., Bergin, S.D., King, P.J., Khan, U., Shvets, I.V., 2011. Science 331, 568–571.
Fadeel, M.A., Crump, J.A., Mahoney, F.J., Nakhla, I.A., Mansour, A.M., Reyad, B., Bibb, W.F., 2004. Am. J. Trop. Med. Hyg. 70, 323–328.
Gao, G., Chen, C., Xie, X., Su, Y., Kang, S., Zhu, G., Cai, L., 2017. Mater. Res. Lett. 5, 267–275.
Hornick, R., Greisman, S.E., Woodward, T.E., DuPont, H.L., Dawkins, A.T., Snyder, M.J., 1970. N. Engl. J. Med. 283, 686–691.
Houwena, F.P., Kageb, A., 2012. Aptamers the Chemical Antibodies. In: Meulenberg, E.P. (Ed.), Antibodies Applications and New Developments, pp. 300–314.
Jayasena, S.D., 1999. Clin. Chem. 45, 1628–1650.
John, J., Van Aart, C.J., Grassly, N.C., 2016. PloS Negl. Trop. Dis. 10, 4616.
Kishore, S., Verma, D., Siddique, M.E., 2014. J. Clin. Diagn. Res. 8, 41.
Kumar, V., Shorie, M., Ganguli, A.K., Sabherwal, P., 2015. Biosens. Bioelectron. 72, 56–60.
Loan, P.T.K., Zhang, W., Lin, C.T., Wei, K.H., Li, L.J., Chen, C.H., 2014. Adv. Mater. 26, 4838–4844.
Looney, R.J., Steigbigel, R.T., 1986. J. Lab. Clin. Med. 108, 498–505.
Marks, R.S., Abdulhalim, I., 2015. Nanomaterials for Water Management: Signal Amplification for Biosensing From Nanocomposites, first ed. Pan Stanford, Boca Raton.
Meirinho, S.G., Dias, L.G., Peres, A.M., Rodrigues, L.R., 2016. Biotechnol. Adv. 34, 941–953.
Mohammed, M., Hello, S., Leekitcharoenphon, P., Hendriksen, R., 2017. BMC Infect. Dis. 17, 544.
Mutreja, R., Jariyal, M., Pathania, P., Sharma, A., Sahoo, D.K., Suri, C.R., 2016. Biosens. Bioelectron. 85, 707–713.
Nayar, N., Shukla, I., Sultan, A., 2014. Int. J. Sci. Res. 4, 1–6.
Pandey, S.K., Rishi, P., Suri, C.R., Vinayaka, A.C., 2015. RSC Adv. 5, 88234–88240.
Pandey, S.K., Suri, C.R., Chaudhary, M., Tiwari, R.P., Rishi, P., 2012. Mol. BioSyst. 8, 1853–1860.
Pandey, S.K., Vinayaka, A.C., Rishi, D.B., Rishi, P., Suri, C.R., 2014. Anal. Chim. Acta 841, 51–57.
Pathania, P., Sharma, A., Kumar, B., Rishi, P., Suri, C.R., 2017. Microchim. Acta 184, 1499–1508.
Rao, C.E.E., Sood, A.E., Subrahmanyam, K.E., Govindaraj, A., 2009. Angew. Chem. Int. Ed. 48, 7752–7777.
Robbins, J.D., Robbins, J.B., 1984. J. Infect. Dis. 150, 436–449.
Sahu, T.S., Mitra, S., 2015. Sci. Rep. 5, 12571.
Sefah, K., Shangguan, D., Xiong, X., Odonoghue, M., Tan, W., 2010. Nat. Protoc. 5, 1169.
Sharma, A., Qadri, A., 2004. Proc. Natl. Acad. Sci. USA 101, 17492–17497.
Sharma, P., Tuteja, S.K., Bhalla, V., Shekhawat, G., Dravid, V.P., Suri, C.R., 2013. Biosens. Bioelectron. 39, 99–105.
Srivastava, R.K., Srivastava, S., Narayanan, T.N., Mahlotra, B.D., Vajtai, R., Ajayan, P.M., Srivastava, A., 2011. ACS Nano 6, 168–175.
Wang, P.P., Sun, H., Ji, Y., Li, W., Wang, X., 2014. Adv. Mater. 26, 964–969.
Wilson, R.P., Winter, S.E., Spees, A.M., Winter, M.G., Nishimori, J.H., Sanchez, J.F., Bäumler, A.J., 2011. Infect. Immun. 79, 830–837.
World Health Organization (WHO), 2017. Typhoid Fever 2016.
Wu, X., Li, Z., Chen, X.X., Fossey, J.S., James, T.D., Jiang, Y.B., 2013. Chem. Soc. Rev. 42, 8032–8048.